

Structure–Activity Relationships in the Acceleration of a Hetero Diels–Alder Reaction by Metalloporphyrin Hosts

Moshe Nakash*^{†,‡} and Jeremy K. M. Sanders*[†]

Cambridge Centre for Molecular Recognition, University Chemical Laboratory, Lensfield Road, Cambridge CB2 1EW, U.K.

jkms@cam.ac.uk

Received June 20, 2000

At 0.33 mM in dichloromethane at 25 °C the cyclic metalloporphyrin hosts **5**, **7**, **8**, and **10** accelerate 12-fold, 260-fold, 1130-fold, and 250-fold, respectively, the reaction of **1** and **2** and also bind the product **3** very strongly. These observations combined with previously measured results with hosts **6**, **9**, and **11** allowed us to explore the influence of host geometry changes on acceleration rates and product binding over a wide range of host molecules of different size, ranging from extremely tightly strapped to very relaxed. To estimate the Zn–Zn distance in the transition-state complex, we carried out quantum mechanical calculations (at the HF/6-31G* level) for the transition state to form **3**. The structure–activity relationships found for hosts **5**–**11**, along with the structural features calculated for the transition-state structure between **1** and **2** and previously crystallographically observed for product-free hosts and for a host–product complex,⁴ suggest that *both* host preorganization as well as host flexibility are key features leading to high acceleration rates and product binding and that it is the delicate balance between the two structural features that leads to maximum efficiency.

Introduction

The long-term goal of supramolecular catalysis is to be able to obtain a catalyst for any given reaction (especially reactions for which there is no known catalyst) with acceleration and regio- and stereocontrol rivalling that of natural enzymes. However, despite the continued development of synthetic methods, allowing the syntheses of ever more complex host molecules, progress to date has been slow. Partly, this is due to the lack of information on how a host's structural features can affect its efficiency in accelerating chemical reactions.¹ The Diels–Alder reaction is a bimolecular process that proceeds through a transition state that resembles the Diels–Alder product,² so achieving turnover is a challenge for biology and the synthetic chemist alike.³ The acceleration and catalysis of Diels–Alder reactions by artificial receptors,^{4–7} antibodies,⁸ and RNA⁹ is well documented.

However, rigorous studies that explore in detail the influence of host geometry changes on acceleration rates and that could shed useful light on the structural features responsible for success or failure are scarce.¹⁰ It is a common view that host rigidity and preorganization are paramount, but kinetic, binding, and crystallographic results for Diels–Alder reactions accelerated by oligoporphyrins suggest that flexibility is important: host responsiveness to the geometrical demands of the guests and transition state is a key factor controlling rate and regioselectivity.^{4,6} In this paper, we report what we believe to be the most comprehensive study of the relationship between synthetic host structure and the ability to accelerate a Diels–Alder reaction.

The regiospecific hetero Diels–Alder reaction of 4-pyridyl butadiene **1** with 3-nitrosopyridine **2** to give oxazine **3** (Figure 1a) can be accelerated by various metallopor-

* To whom correspondence should be addressed. Phone: +44-1223-336411. Fax: +44-1223-336017.

[†] Cambridge Centre for Molecular Recognition.

[‡] Address after 1 Oct 2000: School of Chemistry, Raymond and Beverly Sackler Faculty of Exact Sciences, Tel-Aviv University, Tel-Aviv 69978, Israel. E-mail: nakashm@post.tau.ac.il.

(1) (a) Kirby, A. J. *Angew. Chem., Int. Ed. Engl.* **1996**, *35*, 707. (b) Sanders, J. K. M. *Chem. Eur. J.* **1998**, *4*, 1378.

(2) (a) Sauer, F. K. *Tetrahedron Lett.* **1984**, *25*, 4609. (b) Houk, K. N.; Brown, F. K. *Tetrahedron Lett.* **1984**, *25*, 4609. (c) Houk, K. N.; Gonzalez, J.; Li, Y. *Acc. Chem. Res.* **1995**, *28*, 81.

(3) This may be why there is only one current candidate for a natural Diels–Alderase enzyme: (a) Oikawa, H.; Katayama, K.; Suzuki, Y.; Ichihara, A. *Chem. Commun.* **1995**, 1321. (b) Oikawa, H.; Kobayashi, T.; Katayama, K.; Suzuki, Y.; Ichihara, A. *J. Org. Chem.* **1998**, *63*, 8748.

(4) Nakash, M.; Clyde-Watson, Z.; Feeder, N.; Davies, J. E.; Teat, S. J.; Sanders, J. K. M. *J. Am. Chem. Soc.* **2000**, *122*, 5286.

(5) Marty, M.; Clyde-Watson, Z.; Twyman, L. J.; Nakash, M.; Sanders, J. K. M. *Chem. Commun.* **1998**, 2265.

(6) Clyde-Watson, Z.; Vidal-Ferran, A.; Twyman, L. J.; Walter, C. J.; McCallien, D. W. J.; Fanni, S.; Bampos, N.; Wylie, R. S.; Sanders, J. K. M. *New J. Chem.* **1998**, *22*, 493.

(7) (a) Kang, J.; Santamaria, J.; Hilmersson, G.; Rebek, J. Jr. *J. Am. Chem. Soc.* **1998**, *120*, 7389. (b) Rebek, J. Jr.; Kang, J. *Nature* **1997**, *385*, 50. (c) Ooi, T.; Kondo, Y.; Maruoka, K. *Angew. Chem., Int. Ed. Engl.* **1998**, *37*, 3039. (d) Wang, B.; Sutherland, I. O. *J. Chem. Soc., Chem. Commun.* **1997**, 1495. (e) Hamilton, A. D.; Hirst, S. C. *J. Am. Chem. Soc.* **1991**, *113*, 382. (f) Kelly, T. R.; Meghani, P.; Ekkundi, V. S. *Tetrahedron Lett.* **1990**, *31*, 3381. (g) Breslow, R.; Guo, T. *J. Am. Chem. Soc.* **1988**, *110*, 5613.

(8) (a) Meekeel, A. A. P.; Resmini, M.; Pandit, U. K. *J. Chem. Soc., Chem. Commun.* **1995**, 571. (b) Hilvert, D.; Hill, K. W.; Nared, K. D.; Auditor, M.-T. M. *J. Am. Chem. Soc.* **1989**, *111*, 9261. (c) Schultz, P. G.; Braisted, A. C. *J. Am. Chem. Soc.* **1990**, *112*, 7430. (d) Gouverneur, V. E.; Houk, K. N.; de Pascual-Teresa, B.; Beno, B.; Janda, K. D.; Lerner, R. A. *Science* **1993**, *262*, 204. (e) Yli-Kauhaluoma, J. T.; Ashley, J. A.; Lo, C.-H.; Tucker, L.; Wolfe, M. M.; Janda, K. D. *J. Am. Chem. Soc.* **1995**, *117*, 7041.

(9) (a) Tarasow, T. M.; Tarasow, S. L.; Tu, C.; Kellogg, E.; Eaton, B. E. *J. Am. Chem. Soc.* **1999**, *121*, 3614. (b) Seelig, B.; Jäschke, A. *Chem. Biol.* **1999**, *6*, 167.

(10) (a) For some examples where different metalloporphyrin hosts were used see refs 4–6. (b) For the effect of geometrical changes in ester substrates on the acceleration of acylated reactions induced by β -cyclodextrin see: Breslow, R.; Trainor, G.; Ueno, A. *J. Am. Chem. Soc.* **1983**, *105*, 2739.

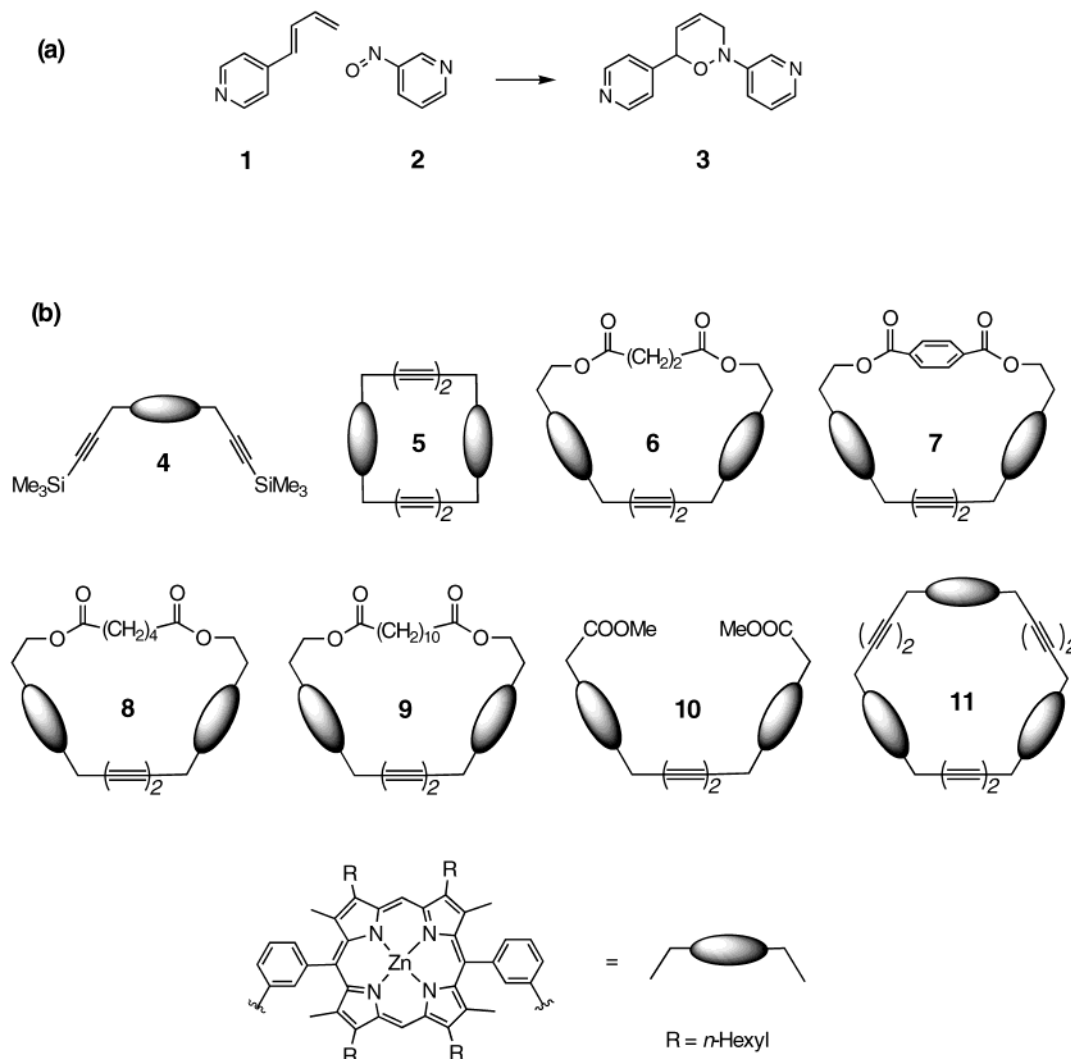


Figure 1. (a) Hetero Diels–Alder reaction of **1** and **2** to give adduct **3**. (b) Structure of porphyrins employed in this work. Synthetic details for **4**,¹⁶ **5**,^{15a} **6**,⁴ **7**,¹² **8**,¹⁶ **9**,¹⁶ **10**,^{15a} and **11**^{15a} have been given previously.

phyrin dimers and trimer, such as **6**,⁴ **9**,⁴ and **11**⁵ (Figure 1b), leading to rate accelerations of 65–840-fold (Table 1). Addition of 2 equiv of monomer **4** (Figure 1b) to a reaction mixture of **1** and **2** leads to an acceleration rate of only 2-fold (Table 1).⁵ This suggests that it is mainly the cyclic structures of these hosts that hold the two reactants in close proximity inside the cavity that leads to the significant acceleration rates observed with these hosts.¹¹ Recently, the X-ray structures of solvated **6**,⁴ **7**,¹² **9**⁴ and of the **6****3** complex⁴ were determined.¹³ As the Diels–Alder product resembles the Diels–Alder transition state,² the structures of the product-free host **6** and the **6****3** host-product complex (Figure 2) allowed, for the first time for synthetic receptors, a detailed structural analysis of the geometrical changes imposed on an accelerating agent on binding of a Diels–Alder product, and confirmed the importance of host flexibility for acceleration of the hetero Diels–Alder (Figure 1a) within the cavity of a cyclic metalloporphyrin receptor.^{4,14} To explore the influence of host geometry changes on acceleration rates over a wide range of host molecules of different size, ranging from extremely tightly strapped to very relaxed, we have now extended our kinetic and binding measurements to a series of dimers including **5**, **7**, **8**, and **10** (Figure 1b). To obtain a reasonable estimate for the host's Zn–Zn distance expected in the transition

state complex of the host-accelerated reactions, we have also carried out ab initio quantum mechanical calculations (at the HF/6-31G* level) for the transition state

(11) (a) The very weak acceleration rate observed with monomer **4** and the fact that addition of 1 equivalent of product **3** to the reaction mixture of **1** and **2** in the presence of **11** strongly inhibits the reaction rate (the acceleration rate is reduced by 20-fold),⁵ suggest that the accelerated reaction in the presence of such cyclic-metalloporphyrin hosts occurs inside the cavity of the host. (b) Free metal cations have also been used to accelerate Diels–Alder reactions (for recent reviews, see: Kagan, H. B.; Riant, O. *Chem. Rev.* **1992**, *92*, 1007; Pindur, U.; Lutz, G.; Otto, C. *Chem. Rev.* **1993**, *93*, 741). However, as the Zn atoms in our systems are coordinated to the pyrrole rings in the porphyrin units, this is expected to reduce the positive charge on the Zn atoms and therefore to reduce their Lewis acidity in comparison with free Zn²⁺ cations. Indeed, the charge on the Zn atom in a Zn-porphyrin unit was calculated to be only +0.4, see: Zerner, M.; Gouterman, M. *Theor. Chim. Acta* **1966**, *4*, 44. Therefore, this is expected to reduce the stabilisation due to acid–base interaction between the pyridine groups and the Zn atoms in our systems, relative to such a stabilisation with free Zn²⁺ cations, and could account for the low acceleration rate (of only 2-fold) observed with monomer **4**. (c) As each of the porphyrin units in hosts **5**–**11** can bind the reactants inside or outside the cavity, only a small fraction of bound host is the reactive complex (host + the two reactants *inside* the cavity) which leads to accelerated product formation. Therefore, the acceleration rates shown in Table 1 underestimates the true ability of such hosts to accelerate the Diels–Alder reaction *inside* the cavity of the host. The kinetic and stoichiometric aspects of the Diels–Alder reaction in the presence of cyclic-metalloporphyrin hosts have been thoroughly discussed elsewhere: Wylie, R. S.; Sanders, J. K. M. *Tetrahedron* **1995**, *51*, 513.

(12) Nakash, M.; Clyde-Watson, Z.; Feeder, N.; Teat, S. J.; Sanders, J. K. M. *Chem. Eur. J.* **2000**, *6*, 2112.

Table 1. Host Accelerated Rates for Formation of **3 and Binding Constants of **3** with Various Hosts, Measured in Dichloromethane at 25 °C**

porphyrin host	Zn–Zn distance ^a (Å)	rate acceleration ^{b,c} (approximate)	binding constant ^d (M ⁻¹)	porphyrin host	Zn–Zn distance ^a (Å)	rate acceleration ^{b,c} (approximate)	binding constant ^d (M ⁻¹)
2 equiv of 4 ^e		2	6.9×10^3	8	12.3 ⁱ	1130	7.6×10^7
5	10.2 ^f	12	2.1×10^6	9 ^g	14.6 ^g	840	7.1×10^7
6 ^g	10.6 ^g	65	5.6×10^7	10	16.6 ^j	250	1.2×10^7
7	11.8 ^h	260	1.1×10^8	11 ^e	15.6 ^k	280 ^l	7.3×10^{6l}

^a Upon the binding of pyridine or MeOH ligands to zinc porphyrins the Zn atom lies above the porphyrin N₄ plane at a mean distance of ~ 0.2 Å (see crystal structures in refs 4, 12, and 30). Therefore, in the host-product complex⁴ and also expected in the transition-state complex, both binding Zn atoms are displaced from the porphyrin N₄ plane (each by ~ 0.2 Å). To allow a more relevant comparison between the Zn–Zn distances in Table 1 and between these values and those in the above complexes, all the values shown are normalized to a case of doubly bound host. This is needed as only one ligand is bound to only one of the porphyrin units in **7**, in contrast to all the crystal structures solved for other hosts in the table, and for which all the porphyrin units bind a ligand. Obviously, this correction is also needed for the cases where molecular models, in which the host is ligand-free, were used to estimate the Zn–Zn distance. See also the footnotes below. ^b Increase in initial rate due to the presence of 1 equiv of host molecule. ^c The control (host-free) reaction was proved to be first order with respect to both the diene and dienophile with a rate constant of $0.0039 \text{ M}^{-1} \text{ s}^{-1}$.⁵ ^d The binding constant of oxazine **3** to trimer **11** corresponds to the initial bidentate interaction of the ligand with the host observed at low oxazine concentrations. ^e See ref 5. ^f Unfortunately, many attempts to obtain appropriate crystals for **5** from different solvent combinations and temperatures were unsuccessful. Due to relatively high structural strain in **5**, as indicated by molecular models that predict a domed shape structure (unconfirmed experimentally) for the porphyrin units in free **5**, and which render calculation of the Zn–Zn distance for that host unreliable, we used the crystal structure of **6**⁴ to estimate this distance. In **6**, the diester linkage is longer than the butadiyne linkage. Therefore, the distance between the two connecting meso carbons which are closer to the diester linkage is 11.6 Å, while that of the two connecting meso carbons which are closer to the butadiyne linkage is only 10.6 Å. As the two porphyrin units in **6** are qualitatively planar (see Figure 2, left and center) and as in **5** both linkages are of the butadiyne type, the distance between the two porphyrin N₄ planes in **5** is estimated to be 10.6 Å. Correction for ligand binding (see footnote a above) leads to the estimated value shown. As molecular models suggest that due to strain the two porphyrin units in **5** might adopt a slightly domed shape, the value of 10.2 Å shown should be regarded as a lower limit. ^g See ref 4. ^h The Zn–Zn distance found in the crystal structure of **7** is 12.045(2) Å.¹² As only one of the porphyrin units in **7** binds a MeOH ligand in this crystal, only one of the Zn atoms in **7** lies above the porphyrin N₄ plane (at a mean distance of ~ 0.2 Å). Therefore, to allow a more relevant comparison between the Zn–Zn distances in the hosts shown in Table 1 and between these values and the Zn–Zn distances in the host-product and transition state complexes, a corrected value for a doubly bound **7** is shown (see also footnote a above). ⁱ Derived from an unpublished crystal structure of **8**. The quality of this X-ray structure is poor, and therefore, it was not possible to elucidate part of this host structure. However, as the Zn atoms in **8** have a relatively large atomic weight, this allows a reliable determination of the Zn–Zn distance in that crystal structure. ^j Calculated from molecular models for the geometry illustrated. Unfortunately, many attempts to obtain crystal structure for **10** from different solvent combinations at different temperatures were unsuccessful. ^k Calculated from molecular models. Similar values were found in an X-ray structure for a complex between two interpenetrating trimers in the solid state.³⁰ Due to this complexation, structural distortions were imposed on each of the two trimers in the complex leading to three somewhat different Zn–Zn distances. Therefore, molecular models were used to calculate the value for a single free undistorted trimer. ^l To allow comparison with host **11**, one has to consider that trimer **11** has six constructive binding possibilities for the diene + dienophile or for oxazine **3**, whereas the hosts **5–10** have only two constructive binding possibilities. Therefore, a trimer should inherently be $6/2 = 3$ times better at accelerating the reaction and binding oxazine **3** than a host molecule that has only two Zn binding sites (as in **5–10**), and to compare the efficiency of the above host molecules, per two Zn binding sites, the acceleration rate and binding constant of host **11** should be divided by three.

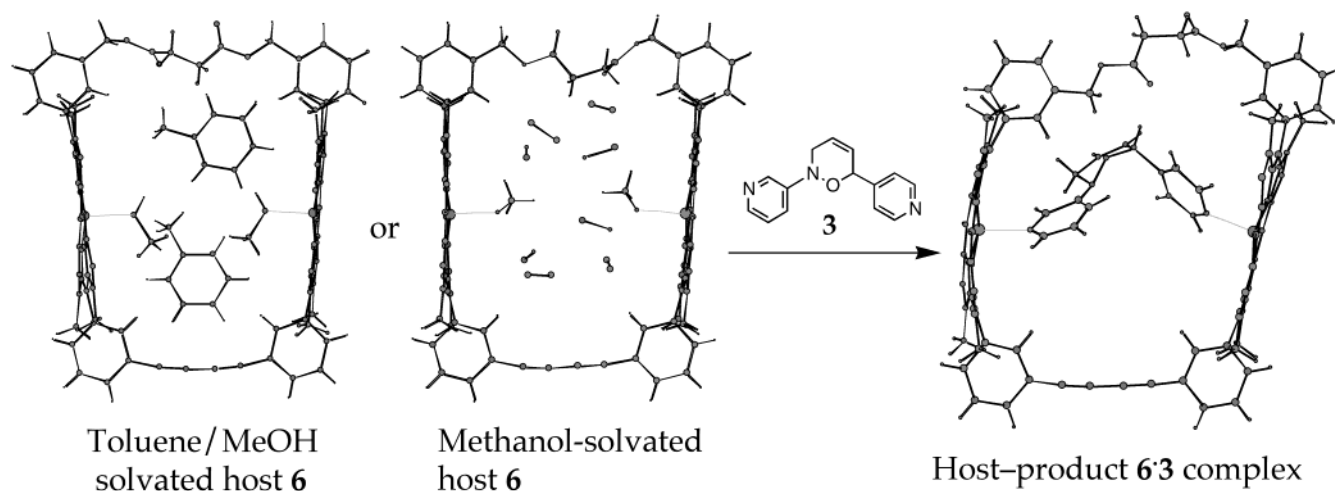


Figure 2. Crystal structures of toluene/MeOH and of MeOH solvated **6** and of the **6-3** complex.⁴ The hexyl side chains (four per porphyrin unit) have been omitted for clarity.

structure between **1** and **2** (Figure 3c) to form **3** (Figure 3a,b). The structure-activity relationships found in the

(13) Growing crystals suitable for X-ray crystallography for these types of relatively large host molecules and which have a large cavity size and long solubilising hexyl chains is not trivial. Unfortunately, many attempts to obtain crystals suitable for X-ray crystallography for the other hosts shown in Figure 1b and their complexes with **3** from different solvents combinations and temperatures were unsuccessful even when synchrotron sources of X-rays were used.

series of hosts **5–11** and the good correlation found between the host-induced acceleration rates and the strengths of product binding by these hosts (Table 1), in conjunction with the structural features calculated for the transition state structure between **1** and **2** (Figure

(14) The aspects of solvent displacement by ligands from the host's cavity and the solvent effects observed for the control (host-free) and host-accelerated reactions are discussed in refs 4 and 5.

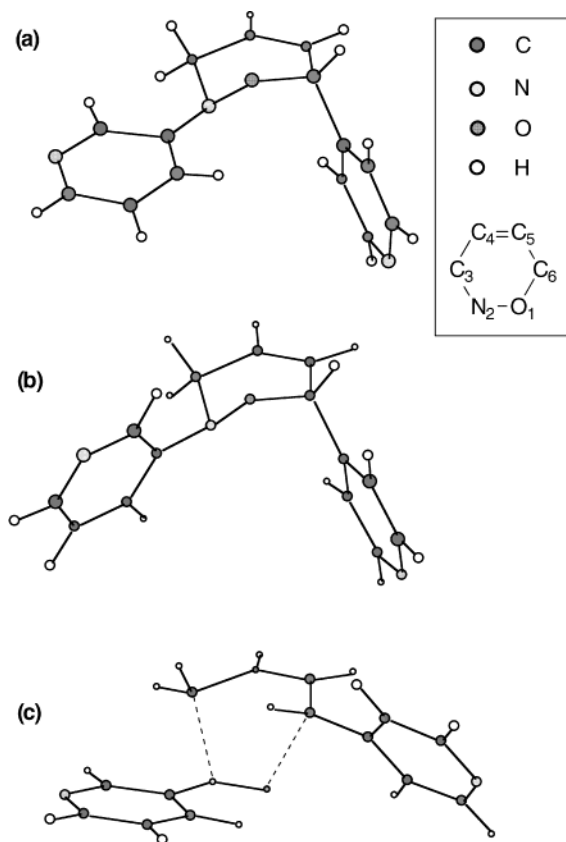


Figure 3. (a) X-ray structure of **3** as found in the **6·3** complex (see Figure 2 – right side).⁴ The N–N distance between the two pyridine nitrogens is 7.52(3) Å. The bond lengths (Å) in the oxazine ring are as follows: O1–N2 = 1.48(2), N2–C3 = 1.36(3), C3–C4 = 1.55(4), C4–C5 = 1.42(4), C5–C6 = 1.42(4), C6–O1 = 1.43(3). (b) Calculated (at HF/6-31G* level) structure of **3**. The N–N distance between the two pyridine nitrogens is 7.497 Å. The bond lengths (Å) in the oxazine ring are as follows: O1–N2 = 1.401, N2–C3 = 1.455, C3–C4 = 1.507, C4–C5 = 1.317, C5–C6 = 1.508, C6–O1 = 1.410. (c) Calculated (at HF/6-31G* level) transition state structure for the reaction between **1** and **2** to form product **3** (Figure 1a). The N–N distance between the two pyridine nitrogens is 8.899 Å. The bond lengths (Å) in the oxazine ring are as follows: O1–N2 = 1.245, N2–C3 = 1.994, C3–C4 = 1.389, C4–C5 = 1.383, C5–C6 = 1.385, C6–O1 = 2.023.

3c) and those found previously in the X-ray structures of product-free hosts and a host·product complex (see Figure 2),⁴ suggest that *both* host preorganization as well as host flexibility are required to obtain high acceleration rates.

Results and Discussion

Synthesis of all the dimers used in this study, **5**,^{15a} **7**,¹² **8**,¹⁶ and **10**,^{15a} (Figure 1b), have been reported previously. These dimers accelerate 12-fold, 260-fold, 1130-fold, and 250-fold, respectively, the reaction of **1** and **2** and also bind the product **3** very strongly (Table 1). This, combined with previously measured results with hosts **6**,⁴ **9**,⁴ and **11**⁵ provide a wide range of kinetic and binding results over a wide range of structurally different hosts.

(15) (a) The general route for linear and cyclic dimers and trimers is described in Anderson, H. L.; Anderson, S.; Sanders, J. K. M. *J. Chem. Soc., Perkin Trans. 1* **1995**, 2231. (b) The procedure of UV/visible titrations is also described in ref 15a.

(16) The general route for hexyl substituted Zn-porphyrins and capped cyclic dimers is described in: Twyman, L. J.; Sanders, J. K. M. *Tetrahedron Lett.* **1999**, 40, 6681.

Examination of the data presented in Table 1 shows an increase followed by a decrease in the acceleration rates and binding constants in the series of hosts **5–11**. The good correlation found between the host-induced acceleration rates and the binding constants between these hosts and the Diels–Alder product **3** can be attributed to the resemblance² of the Diels–Alder product to the Diels–Alder transition state (see Figure 3). This correlation indicates that **3** is a reasonable transition state analogue for the reaction in Figure 1a and reinforces our previous conclusions on the type of structural distortion expected in the transition-state complex, implied by comparing the X-ray structures of the product-free host **6** and the **6·3** complex (Figure 2).⁴

However, deviation from the above correlation is also apparent (Table 1): the best accelerating agent is host **8** while host **7** shows the strongest binding constant with **3**. To gain understanding of this difference, we have carried out *ab initio* quantum mechanical calculations (at the HF/6-31G* level) for **3** (Figure 3b) and for the transition state to form **3** (Figure 3c). For comparison, the X-ray structure of **3**, determined as a complex with **6**,^{4,17} is also shown in Figure 3a. Although the Diels–Alder product resembles its transition state, the calculations reveal distinct structural differences between the two, among which the most relevant to our study is the different conformation adopted by the oxazine ring in these structures (Figure 3).¹⁸ This leads to different N–N distances between the two pyridine nitrogens: 7.5 Å in **3** and 8.9 Å in the transition state structure to form **3** (Figure 3). This, in addition to the two Zn–N distances in the transition state complex, approximated to be as in the **6·3** complex (~2.2 Å),⁴ provides an estimated distance of 13.3 Å between the two zinc atoms in the transition state complex, rather than the 11.7 Å¹⁹ that was found in the crystal structure for the **6·3** complex.⁴ This could account for the observation that the host that shows the strongest binding constant with **3** is not the best accelerating agent (Table 1); the highest acceleration rate is observed for host **8**, which has the closest Zn–Zn distance to that expected in the transition state complex

(17) **3** is a viscous oil and attempts to obtain crystals for an unbound oxazine **3** from different combinations of solvents and temperatures were unsuccessful.

(18) Less significant structural differences are expected between the transition state and product in Diels–Alder reactions which form bicyclo[2.2.2]octene systems. In such systems the ethano bridge locks the cyclohexene ring in the product (in contrast to the flexible oxazine ring in **3**) in a conformation that more closely resembles the proposed pericyclic transition state² for the Diels–Alder reaction of a cisoid diene and dienophile. This is the reason for the use of such systems as haptens in the generation of catalytic antibodies.^{8a–d} For a structural study of such haptens see: Gouverneur, V. E.; Houk, K. N.; de Pascual-Teresa, B.; Beno, B.; Janda, K. D.; Lerner, R. A. *Science* **1993**, 262, 204.

(19) A similar value of 11.9 Å can be calculated from the N–N distance between the two pyridine nitrogens in **3** (of 7.5 Å, see Figure 3a–b) + the two Zn–N distances found in the X-ray structure of the **6·3** complex (~2.2 Å each⁴). This small difference (of 0.2 Å) between the value calculated and that found experimentally in the **6·3** complex (11.7 Å⁴) results from the orientation of the pyridine rings and lone pairs in **3** relative to the Zn sites in **6**. In particular, the N_{py}–Zn–Zn angles are 5.2(6)° and 21.3(4)° for the 3- and 4-pyridine, respectively (see Figure 2, right side). As the orientation of **3** in the cavity of **6** leads to only a small difference (0.2 Å) between the experimental and calculated Zn–Zn distance in the **6·3** complex, and as in the transition state structure to form **3** (Figure 3c) the pyridine rings are oriented in a way that the two nitrogens lone pairs are qualitatively directed to opposite directions (while this is not the case for **3**, see Figure 3a,b) and which therefore is expected to lead to a smaller N_{py}–Zn–Zn angles in the transition state complex, give additional confidence to the calculated value of the Zn–Zn distance expected in the transition state complex (of 13.3 Å, see text).

of 13.3 Å, while the strongest binding constant is obtained with host **7**, which has the closest Zn–Zn distance to that observed in a host-product complex of 11.7 Å (as in the **6·3** complex, Figure 2). This finding indicates that host preorganization, i.e., a Zn–Zn distance that is close to that expected in the transition state complex, is an important feature leading to higher host-induced acceleration rates and stronger binding constants between cyclic metaloporphyrin hosts and a bidentate ligand such as **3**.

The oxazine ring in the calculated structure of **3** (Figure 3b) has a similar structure to that found experimentally for **3** (Figure 3a) in the **6·3** complex.^{4,20,21} The main difference between the two structures of **3** is the different degree of rotation of the 3-pyridine ring with respect to the oxazine ring (see Figure 3a,b). This difference results from the need of the pyridine rings in the X-ray structure of **3** (Figure 3a) to adopt the necessary rotation angles to optimize binding inside host **6** (see Figure 2, right side),⁴ while the calculations were performed for an unbound **3**. Similar N–N distances of 7.52(3)⁴ and 7.50 Å,²² respectively, were found between the two pyridine nitrogens in the X-ray structure (Figure 3a) and the calculated structure (Figure 3b) of **3** although the 3-pyridine ring in these structures is rotated to a different extent. The similar conformation and structure adopted by the oxazine ring in the X-ray structure and calculated structure of **3**, as well as the good agreement found between the bond lengths in these two structures (Figure 3a,b), add credibility to the level of calculations used.²³ As expected, in the transition state, the bond lengths of the forming C6···O1, C3···N2 and C4=C5 bonds are longer while the breaking N2=O1, C3=C4, and C5=C6 double bonds are shorter than the corresponding bonds in the product **3** (see Figure 3b,c).

In addition to the importance of host preorganization (see above), the results in Table 1 also suggest that host flexibility and responsiveness to the geometrical demands of the transition state are a key factors controlling acceleration rates. The smallest and the most rigid host **5**, among the host molecules used in this study (Figure 1b), has a relatively short Zn–Zn distance of 10.2 Å (Table 1), shorter by 1.5 Å than the 11.7 Å found in a host-product complex (see Figure 2) and shorter by 3.1 Å than the 13.3 Å expected in the transition state complex (see above). The rigidity built into host **5**, due to its two butadiyne linkages, reduces its ability to distort its structure upon binding of relatively large bidentate

ligands. This increases the energetic cost of binding **3** and even more so with the transition state to form **3**. This accounts for the lower binding constant with **3** and the relatively poor acceleration rate of only 12-fold observed with host **5** (Table 1). In contrast to **5**, host **6**, which has a Zn–Zn distance of only 0.4 Å longer than in **5** (Table 1) but which has a more flexible connecting diester linkage than the two butadiyne linkages in **5**, shows a much stronger binding constant with **3** and a more significant acceleration ability, of 65-fold (Table 1). Although the Zn–Zn distance in the free host **6** (10.576(5) Å, Figure 2, left side) is much shorter than in the **6·3** complex (11.684(3) Å, Figure 2, right side) and even more so than the expected distance in the transition state complex, the ability of host **6** to distort its structure, as can be seen by comparing the structures of the product free host **6** and the **6·3** complex (Figure 2),²⁴ is responsible for the observation that it binds **3** very strongly and is able to accelerate effectively the reaction of **1** and **2** (Table 1).^{4,25} Therefore, if **6** was unable to distort its structure it would be less effective in stabilizing the transition state complex and in accelerating the reaction in Figure 1a. Obviously, flexible host molecules with a longer Zn–Zn distance, closer to that in the transition state complex, are expected to be better in accelerating the reaction in Figure 1a. Indeed, the relatively flexible hosts **7**, **8** and **9** which have Zn–Zn distances of 11.8, 12.3, and 14.6 Å, respectively (Table 1), show much improved acceleration rates of 260-fold, 1130-fold and 840-fold respectively (Table 1), the most efficient host (**8**) being the one that has the closest Zn–Zn distance to that expected in the transition state complex (Table 1). A further increase in the Zn–Zn distance, increasing the deviation from that in the product-host or transition state complexes on going from host **8** to host **11**, reduces the binding constants with **3** or the acceleration rates observed (Table 1), demonstrating the importance of host preorganization for successful binding and acceleration.

The linear dimer **10** is found to be anomalous being a good accelerator despite having the biggest deviation from the Zn–Zn distances in the product-host or transition state complexes. Given the large Zn–Zn distance in **10**, which is an underestimate due to free rotation around its butadiyne linkage, and which is expected to increase the entropic cost in organising the host upon binding of **3** or the transition state, the open chain **10** is remarkably effective adding to the evidence that flexibility and responsiveness are important for binding and acceleration. For example, although the Zn–Zn distances in **10** deviates by 3.3 Å from that expected in the transition state complex, while host **7** deviates by only 1.5 Å, both hosts **7** and **10** induce similar acceleration rates (Table 1). The ability of **10** to accelerate so well the reaction in Figure 1a surely reflects its ability to adjust to the correct transition state geometry. This could also account for the observation that a linear dimer such as **10** is also efficient

(20) The possible geometries of **3** were explored by a Monte Carlo conformational search and were optimised. The most stable structure for **3** has the same conformation for the oxazine ring and the same type of inversion about the nitrogen atom in this ring as was found in the **6·3** crystal structure.

(21) For a theoretical study of hetero-Diels–Alder reactions, see: Park, Y. S.; Lee, B.-S.; Lee, I. *New J. Chem.* **1999**, *23*, 707.

(22) The N–N distance of 7.50 Å calculated now for **3** with the ab initio quantum mechanical calculations method (at the HF/6-31G* level) is more reliable than the value of 8.1 Å obtained previously⁴ with the lower quality force field method (using the UNIVERSAL 1.02 force field). The discrepancy between these two values results from the different rotation of the 3-pyridine ring with respect to the oxazine ring in these structures.

(23) The main motivation in calculating the structures in Figure 3 was to obtain a reliable N–N distance in the transition state to form **3**, and from which an estimate for the Zn–Zn distance in the transition state complex could be obtained (see text). Obviously, minor changes in bond lengths for the structures shown in Figure 3 would not cause a significant change in the overall N–N distance. Therefore, more sophisticated and expensive levels of calculations were not employed for these types of relatively large molecules.

(24) Comparison of the solvated rectangle-like structures of the product-free host **6** (Figure 2, left and center) with the **6·3** complex (Figure 2, right side) reveals that when the Diels–Alder product **3** is bound within the cavity, it induces structural changes in **6**: the two porphyrin moieties are pushed apart, increasing the Zn–Zn distance by 1.1 Å; the right-hand porphyrin is forced to lean away from the cavity while remaining virtually planar; and the left-hand porphyrin adopts a domed shape and a slight lean toward the cavity.⁴

(25) There are other examples where flexibility has also been invoked as a key feature of catalytic success: Menger, F. M.; Ding, J.; Barragan, V. *J. Org. Chem.* **1998**, *63*, 7578.

in accelerating with remarkable exo selectivity the Diels–Alder reaction developed previously in our group.^{6,26}

It is also interesting to compare the results observed for hosts **10** and **11** (Table 1). To allow comparison with host **11** one has to consider that trimer **11** has six constructive binding possibilities for the diene + dienophile or for oxazine **3**, whereas hosts **5–10** have only two constructive binding possibilities. Therefore, trimer **11** should inherently be $6/2 = 3$ times better at accelerating the reaction and binding oxazine **3** than a host molecule that has only two Zn binding sites (as in **5–10**). To compare the efficiency of hosts **5–10** with that of **11**, per two Zn binding sites, the acceleration rate and binding constant of host **11** should be divided by three. Although the Zn–Zn distances in Table 1 suggest that **11** is better preorganized for binding **3** and the transition state (in Figure 3c) than **10**,²⁷ it is the more flexible open chain **10** which is more efficient in binding the product **3** and in accelerating the reaction in Figure 1a; $1.2 \times 10^7 \text{ M}^{-1}$ and 250-fold, respectively, while these values are only $2.4 \times 10^6 \text{ M}^{-1}$ and 93-fold, respectively, for trimer **11** (Table 1).²⁸ Again, as in dimer **5**, the rigid butadiyne linkages in **11** are responsible for the lower ability of this host (per two Zn binding sites), in comparison with **10**, to accelerate the reaction in Figure 1a. These results suggest that in order to achieve maximum binding and acceleration efficiency, a balance between host flexibility and preorganization should be introduced to the host structure. Obviously, extremely flexible linkages in hosts will reduce dramatically the host's preorganization, abolishing efficient binding and acceleration abilities. Indeed, kinetic studies on the Diels–Alder reaction developed previously in our group⁶ have illustrated that hydrogenation of the butadiyne or acetylene links in various porphyrin-based hosts leads to almost complete loss of the rate acceleration. Not surprisingly, it appears that too much conformational freedom in the host results in the bound substrates not spending a high enough proportion of time in productive orientations which make the cycloaddition reaction favorable.

Conclusions

In this study we have explored the influence of host geometry changes on host-induced acceleration rates and product binding over a wide range of host molecules of different size and ranging from extremely tightly strapped to very relaxed. The structure–activity relationships found, along with the structural features calculated for the transition state structure between **1** and **2** and found crystallographically for product-free hosts and for a host-product complex,⁴ lead us to conclude that *both* host preorganization as well as host flexibility and responsiveness are key features leading to high acceleration rates and to strong bidentate ligand binding, and it is the delicate balance between these structural features that lead to maximum efficiency.

(26) For a review on linear “foldamers” with remarkably well defined solution conformations, see: Gellman, S. H. *Acc. Chem. Res.* **1998**, *31*, 173.

(27) The Zn–Zn distance in trimer **11**, of 15.6 Å (Table 1), is closer to the Zn–Zn distances in the host-product complex (11.7 Å, see text) and in the transition state complex (13.3 Å, see text), than in host **10** for which the Zn–Zn distance is 16.6 Å (Table 1).

(28) The values used here for trimer **11** are corrected for the statistical factor (see text) and therefore are three times smaller than those shown in Table 1.

Experimental and Computational Section

Kinetic Studies. The control (host-free) Diels–Alder reaction between diene **1** and dienophile **2** was monitored by ¹H NMR in deuteriodichloromethane and in toluene-*d*₈, and showed clean transformation of the starting substrates to the oxazine without significant formation of side products. Monitoring the reaction with ¹H NMR, GC, or HPLC gave similar results. However, GC was the preferred analytical technique for host-accelerated kinetic investigations using 0.5 equivalents of biphenyl as an internal standard. Accelerated reactions were initiated by addition of the host and reaction progress was monitored by HPLC (normal phase 8 × 225 mm Spheres S5W column) or GC (5% dimethyldiphenyl siloxane 25 m × 0.32 mm × 0.25 μm column). For all the reactions the decrease in concentration of diene and dienophile was monitored. After completion of the host-accelerated reactions a few drops of TFA were added to the reaction mixture to demetallate the porphyrin hosts. The oxazine product was thus released from the cavity and could then be detected by HPLC, confirming that the disappearance of the starting substrates correlates directly with oxazine formation. In a typical reaction, diene **1**, dienophile **2** and host were mixed in equimolar amounts, each at a concentration of 0.333 mM and were carried out at 25 °C in dichloromethane. Specific conditions used with HPLC: gradient: 0–10 min EtOAc/MeOH = 100:0, 10 min – end EtOAc/MeOH = 90:10; flow rate: 1 mL/min; stop time: 7 min (fast kinetics), 15 min (slow kinetics); post time: 4 min (fast kinetics), 5 min (slow kinetics); injection volume: 2 μL, draw speed: 200 μL/min; eject speed 200 μL/min; draw position: 0.0 mm; wavelengths used: 298 nm, 302 nm and 306 nm; retention times: dienophile **2**: 2.8 min, diene **1**: 5.4 min, oxazine **3**: 8.4 min. Specific conditions used with GC: program: 110 °C (2 min), 40 °C/min, 250 °C (4.5 min); flow rate 3 mL/min; run time: 10 min; acquisition time: 1 min; injection volume: 0.8 μL; detector: FID; retention times: dienophile **2**: 2.0 min, diene **1**: 3.5 min, oxazine **3**: 7.3 min.

Binding Studies. To gauge the affinity of the substrates and product to the various hosts, a series of UV/visible titrations were carried out at 25 °C in dichloromethane using a Hewlett-Packard 8452A diode array spectrometer fitted with a temperature controlled jacket (estimated error in temperature ±0.1 °C). Other experimental details and data analysis were as described previously.^{15b}

Computational Methods. Molecular orbital calculations were carried out using standard ab initio methods as implemented in the CADPAC²⁹ program. The geometries of product **3** and the transition state (Figure 3b,c) were optimized using restricted Hartree–Fock theory and the 6-31G* basis set. All structures were verified to be either minima or transition state by their Hessian matrixes, which have either zero (minima) or one (transition state) imaginary frequency. The possible geometries of **3** were explored by a Monte Carlo conformational search and were optimized.

Acknowledgment. This work was supported by the EPSRC, British Council, Israel Academy and Ministry of Science, and B'nai B'rith.

Supporting Information Available: Calculated energies and Cartesian coordinates for **3** and for the transition state to form **3** and full structures of hosts **4–11**. This material is available free of charge via the Internet at <http://pubs.acs.org>.

JO0009371

(29) CADPAC: The Cambridge Analytic Derivatives Package Issue 6, Cambridge, 1995. A suite of quantum chemistry programs developed by R. D. Amos with contributions from Alberts, I. L.; Andrews, J. S.; Colwell, S. M.; Handy, N. C.; Jayatilaka, D.; Knowles, P. J.; Kobayashi, R.; Laidig, K. E.; Laming, G.; Lee, A. M.; Maslen, P. E.; Murray, C. W.; Rice, J. E.; Simandiras, E. D.; Stone, A. J.; Su, M.-D.; Tozer, D. J.

(30) Anderson, H. L.; Bashall, A.; Henrick, K.; McPartlin, M.; Sanders, J. K. M. *Angew. Chem., Int. Ed. Engl.* **1994**, *33*, 429.